Final Report for ONR CODE 30 SAAET Program

1. "Understanding Chemical Sensitivity and Surface Response in Detecting Trace Levels of Explosives Using Vibrational Sum Frequency Spectroscopy"
2. **Prime Offeror:** Applied Physics Laboratory, University of Washington
3. **Subcontractors:** none
4. **Period of Performance: 06/01/2009 – 08/30/2013**
5. **Submitted by: William E. Asher, asher@apl.washington.edu, 206-543-5942**
6. **Business Contact: Lynette Arias, Director, University of Washington Office of Sponsored Programs, osp@uw.edu**

7. Background/Scope of Effort

Stand-off detection of trace levels of explosives would be of great benefit in identifying the location of hidden explosive devices and locations where these munitions are assembled. Previous Code 30-sponsored research investigated the use of the nonlinear optical technique vibrational sum frequency spectroscopy (VSFS) for stand-off detection of trace levels of explosives on surfaces. VSFS can detect 2,4,6-trinitrophenol (picric acid), 2,4,6-trinitrotoluene (TNT) and 1,3,5-trinitro-1,3,5-triazacyclohexane (RDX) at surface concentrations as low as 300 ng cm^{-2}. Because these surface concentrations are typical of what might be found on surfaces containing adventitious contamination of explosives [*Stott et al.*, 1994], these laboratory results indicate that VSFS could be used as a remote-sensing probe for detecting trace levels of explosives. However, in order for a method to be useful for operation detection of explosives, it must be demonstrated that the signal generated by explosives can be detected in the presence of environmental contamination on a variety of substrates.

The objectives of the work proposed were to understand the nonlinear optical response of explosives on surfaces that are typically encountered in urban environments, determine if environmental contaminants produce signatures that would mimic those from explosives, and demonstrate that VSFG signals can be detected at stand-off distances of up to five meters.

8. Summary/Abstract

Vibrational sum frequency spectroscopy (VSFS) can be used to detect trace quantities of high explosives (HEs) adsorbed on surfaces. As a trace detection method, VSFS has the advantages of being non-contact and non-destructive with sub-second detection times. Therefore, a HE-detection method for detecting IEDs or portal defense that was based on VSFS could provide stand-off trace detecting for IEDs and increase the throughput of package screening (in terms of objects scanned per minute) for portal defense. Furthermore, because VSFS does not degrade contaminants on surfaces, a positive detection result leaves any explosives detected in place for subsequent forensic analysis such as fingerprint identification. This research has shown that that VSFS provides high chemically selectivity for nitro-containing HEs in the presence of environmental chemical contamination.

9. Technical Contents and Accomplishments

Summary of Results

Experiments conducted under our SAAET project have demonstrated:

1. The VSFS response of nitro-containing explosive crystals adsorbed on surfaces is largely independent of surface contamination or chemical complexity.

2. Range-insensitive optical configurations for performing VSFS measurements are possible and detection using the method at stand-off distances of up to 2.2 m has been demonstrated.
3. Detection time using VSFS is rapid, and it has been demonstrated the method can detect trace levels of urea from suitcases moving on a baggage carousel.
4. In the case of RDX, preparation of samples via recrystallization from solvents produces different crystal structures than found in operational explosive samples, and this affects VSFS signal response.

These results are discussed in detail in the following section.

Technical Background and Discussion of Prior Results

The threat of improvised explosive devices (IEDs) to human life is grave and countering this threat is a high priority for force protection during military operations. Remote, stand-off detection of in-place IEDs would be a significant step forward in mitigating the threat posed by these weapons. Because of the low vapor pressures of most high explosives (HEs) [*CREPSEDT*, 2004], it is extremely difficult to detect their presence in the gas phase using methods that might be adapted as stand-off systems. For example, although cavity ring-down laser spectroscopy (CRLS) has the sensitivity to detect explosives in the gas phase [*Fidric et al.*, 2003], it is not amenable to stand-off application [*CREPSEDT*, 2004]. However, explosives are known to adsorb on surfaces due to their high electronegativity and low vapor pressure [*CREPSEDT*, 2004], and methods relying on detecting their presence on surfaces show promise for remote-sensing applications.

Optical sum-frequency generation (SFG) has long been used for studying surface chemistry [*Lambert et al.*, 2005; *Shen*, 2000]. SFG is a second-order two-photon-mixing process, where the nonlinear interaction between the electromagnetic dipole of a molecule and two incident photons with frequencies ω_1 and ω_2, respectively, leads to the generation of a photon with frequency equal to $\omega_S = \omega_1 + \omega_2$. As a concrete example of this process, when photons having wavelengths of 1064 nm and 532 nm illuminate the surface of urea crystals, photons with wavelengths of 355 nm (in the ultraviolet spectral region) can be detected.

Theoretical considerations show that to a first approximation, sum-frequency generation (SFG) emissions occur only from the surface of an isotropic material such as metals, liquids, or glasses [*Shen*, 1984; 1999]. Furthermore, it has been shown that SFG has the capability to detect sub-monomolecular coverage of molecules adsorbed on surfaces [*Shen*, 2000]. Given the likelihood that HEs will be present on surfaces at low concentrations, surface selectivity and high sensitivity to surface chemistry are key advantages of VSFS in detecting HEs.

The number of photons generated at ω_S is a function of the incident light intensity, the nonlinear optical properties of the material, and the presence of any resonances between vibrational molecular energy transitions and the energy of the incident or outgoing photons [*Shen*, 2000]. This dependence is expressed in terms of the total second order nonlinear polarization of the surface $P^{(2)}$. It can be shown that the SFG intensity is proportional to the three orthogonal components of $P^{(2)}$ at frequency ω_S, which are given by [*Lambert et al.*, 2005]

$$P_i^{(2)}(\omega_S) = \varepsilon_0 \sum_j \sum_k \chi_{ijk}^{(2)} E_j(\omega_1) E_k(\omega_2) \tag{1}$$

where ε_0 is the vacuum permittivity, $\chi_{ijk}^{(2)}$ is the i'th, j'th, k'th component of the second order surface nonlinear response tensor of the system, $\chi^{(2)}$, and $E_j(\omega_1)$ and $E_k(\omega_2)$ are the j'th and k'th

components, respectively, of the electromagnetic fields of the incident laser beams at frequencies ω_1 and ω_2, respectively.

In order to calculate signal intensities, the macroscopic nonlinear surface susceptibility, $\chi^{(2)}$, must be related to the nonlinear polarizability of the individual molecules adsorbed on the surface, $\beta^{(2)}$, and to the polarizability of the surface itself. In general the elements of $\chi^{(2)}$ will not be identical to the elements of $\beta^{(2)}$, and molecular symmetry and orientation will be important in determining the overall nonlinear optical response of the system [*Lambert et al.*, 2005]. In relation to VSFS, it is the behavior of $\beta^{(2)}$ when the frequency of one of the incoming laser beams is near the frequency of a vibrational band that is most important. Near a molecular vibrational mode with frequency ω_v, when $\omega_1 >> \omega_v$ it can be shown that $\beta^{(2)}$ can be estimated from the Raman and vibrational transition moments using [*Hunt et al.*, 1987]

$$\beta_{\alpha\beta\gamma} = \frac{1}{2\hbar}\frac{M_{\alpha\beta}A_{\gamma}}{\left(\omega_v - \omega_2 - i\Gamma\right)} \tag{2}$$

where $M_{\alpha\beta}$ is the Raman transition moment, A_γ is the IR transition moment, ω_2 is the frequency of the incoming IR beam, and Γ^{-1} is the relaxation time of the excited state. Eq. (2) shows that a general selection rule of VSFS is that for a particular vibrational transition to be resonant for SFG, it must be active as both a Raman and an IR band. However, Eq. (2) also shows that the SFG signal arising from the surface polarization can increase by orders of magnitude when $\omega_2 = \omega_v$. Because vibrational transitions of organic molecules occur mainly at IR wavelengths, for VSFS the wavelength of one incoming laser beam must be tunable in the IR region. Because the VSFS response of explosives was unknown, the research conducted for our current ONR-CIED project focused in part on determining whether commonly encountered explosives have nonlinear optical responses that are high enough that would allow VSFS to be used to detect trace levels of HEs, whether there are vibrational bands of explosives that can be used for remote sensing applications, and whether the interaction between the SFG response of the surface itself will degrade the SFG response of HEs adsorbed on the surface.

The nonlinear surface polarization described by Eq. (1) is given in terms of the induced surface-bound electrical field. Although that relation completely defines the sum-frequency generation process, for a given set of experimental conditions it is somewhat simpler to define the process in terms of the intensities of the incoming photons and the effective second-order nonlinear susceptibility, $\chi^{(2)}_{\text{eff}}$ [*Wang et al.*, 2005; *Zhuang et al.*, 1999]. Using this formalism, the intensity of the SFG light emitted from a surface is given by[*Wang et al.*, 2005; *Zhuang et al.*, 1999]

$$I_{\text{SF}} = \frac{8\pi^3\omega_{\text{SF}}^2 \sec^2\theta_{\text{SF}}}{c^3 n_{\text{AIR}}\left(\omega_{\text{SF}}\right) n_{\text{AIR}}\left(\omega_1\right) n_{\text{AIR}}\left(\omega_2\right)}\left|\chi^{(2)}_{\text{eff}}\right|^2 I\left(\omega_1\right) I\left(\omega_2\right) \tag{3}$$

where c is the speed of light in a vacuum, $I(\omega_i)$ is the intensity of the incoming light at ω_i, and $\chi^{(2)}_{\text{eff}}$ is the effective nonlinear susceptibility defined as[*Wang et al.*, 2005; *Zhuang et al.*, 1999]

$$\chi^{(2)}_{\text{eff}} = \left[\hat{e}\left(\omega_{\text{SF}}\right)\cdot\mathbf{L}\left(\omega_{\text{SF}}\right)\right]\cdot\chi^{(2)}_{ijk} : \left[\hat{e}\left(\omega_1\right)\cdot\mathbf{L}\left(\omega_1\right)\right]\left[\hat{e}\left(\omega_2\right)\cdot\mathbf{L}\left(\omega_2\right)\right] \tag{4}$$

where $\hat{e}\left(\omega_i\right)$ is the unit surface electric field vector for photons with frequency ω_i and the elements of $\mathbf{L}(\omega_n)$ are defined as[*Wang et al.*, 2005; *Zhuang et al.*, 1999]

$$L_{xx}(\omega_i) = \frac{2n_1(\omega_i)\cos\phi_i}{n_1(\omega_i)\cos\phi_i + n_2(\omega_i)\cos\theta_i} \tag{5}$$

$$L_{yy}(\omega_i) = \frac{2n_1(\omega_i)\cos\theta_i}{n_1(\omega_i)\cos\theta_i + n_2(\omega_i)\cos\phi_i} \tag{6}$$

$$L_{zz}(\omega_i) = \frac{2n_2(\omega_i)\cos\theta_i}{n_1(\omega_i)\cos\phi_i + n_2(\omega_i)\cos\theta_i}\left(\frac{n_1(\omega_i)}{n'(\omega_i)}\right)^2 \tag{7}$$

where the x and z directions define the plane of the incident laser beams and the reflected sum-frequency photons and $n'(\omega_i)$ is the refractive index of the interfacial layer as defined by *Zhuang et al.*[1999] Equations (5), (6), and (7) can be used to expand Eq. (4) in terms of the specific elements of $\chi^{(2)}$ that will contribute to the SFG signal for a given scattering geometry and polarization configuration of the incoming and reflected SFG beams.

In the special case of SFG configurations using a nadir geometry, all θ_i are equal to zero. This leads to a relatively simple form for $\chi^{(2)}_{eff}$ since both s and p polarizations lie in the plane of the surface and all elements of $\chi^{(2)}$ containing a z component of an electrical field unit vector will be zero (i.e., they contain $\sin(\theta_i)$ with $\theta_i = 0$). Therefore, for each polarization combination of the two incoming beams, pp, ss, ps, and sp (defined so that p polarization is collinear with the x-axis and s is collinear with the y-axis), only two elements of $\chi^{(2)}$ will contribute to the signal. For the polarization combinations ss and ps, $\chi^{(2)}_{eff}$ is given by

$$\chi^{(2)}_{eff}(ss) = L_{yy}(\omega_{SF})L_{yy}(\omega_1)L_{yy}(\omega_2)\chi^{(2)}_{yyy} - L_{xx}(\omega_{SF})L_{yy}(\omega_1)L_{yy}(\omega_2)\chi^{(2)}_{xyy} \tag{8}$$

$$\chi^{(2)}_{eff}(ps) = L_{yy}(\omega_{SF})L_{xx}(\omega_1)L_{yy}(\omega_2)\chi^{(2)}_{yxy} - L_{xx}(\omega_{SF})L_{xx}(\omega_1)L_{yy}(\omega_2)\chi^{(2)}_{xxy} \tag{9}$$

where it should also be noted that in a nadir geometry the two additional polarization configurations, sp and pp, have functional forms that are identical to Eqs. (8) and (9) but with y substituted for x and vice versa. Because the only elements of $\chi^{(2)}$ that are nonzero for isotropic interfaces have a z component,[*Wang et al.*, 2005; *Zhuang et al.*, 1999] Eqs. (8) and (9) also show that nadir optical configurations require planar nonisotropic surfaces to generate SFG signals. This implies that stand-off geometries would not be particularly useful for study of most common liquid surfaces. This result is consistent with the theoretical work done by Gan et al.[2007] showing that the SFG signal intensity from the surface of liquid methanol decreases to zero as incidence angle decreases to zero. The effectiveness and utility of VSFS as a stand-off probe would be greatly compromised if explosives display similar behavior with respect to signal intensity as a function of beam incidence angle.

Many explosives (*e.g.*, TNT, RDX, HMX) contain multiple nitro (-NO_2) groups, and the vibrational modes of -NO_2 are known to have large $\chi^{(2)}$ [*Heinz et al.*, 1983]. In particular, the symmetric stretch of -NO_2 occurs in the mid-wave IR region at a wavenumber of approximately 1325 cm^{-1}, corresponding to a wavelength of 7.55 μm. Figure 1 shows a plot of the SFG signal intensity in arbitrary units, I_{SFG}, of the symmetric stretch of -NO_2 of three explosives: picric acid, RDX, and TNT measured on a fused silica substrate plotted versus surface concentration. Also shown on Figure 1 is I_{SFG} for *p*-nitroaniline (PNA). The data show that I_{SFG} is above the detection

threshold at concentrations of a few hundred nanograms per square centimeter in the case of TNT and significantly lower concentrations for RDX and picric acid. Furthermore, I_{SFG} of the three explosives, while being less than that of PNA as a function of concentration, are still significant in comparison. This is important because PNA has an extremely high $\chi^{(2)}$ [*Zyss*, 1993], so the data in Figure 1 show that $\chi^{(2)}$ for explosives, while not being as high as PNA, are still quite large (in comparison, I_{SFG} for 2-propanol was 1.23 at a surface concentration of 1000 μg cm^{-2}). Figure 1 demonstrates that explosives containing nitro groups have large $\chi^{(2)}$ and can be detected at low surface concentrations using VSFS. However, these data show sum-frequency response in the best-case scenario where the substrate is inactive optically and inert chemically.

The nonlinear susceptibility of both the surface and the adsorbed molecules on the surface play a role in determining I_{SFG} [*Lambert et al.*, 2005]. Because of the interaction of the adsorbate and substrate, successful application of SFG as a molecular probe requires knowledge of the nonlinear optical response of both the target compound and potential substrates. Therefore, the second objective for our ONR CIED work has been to understand the effect of substrate on I_{SFG} for HEs. For example, Figure 2 shows VSFS spectra for the symmetric stretch of RDX fused silica, gold, polished and unpolished T6061 aluminum alloy, unpolished cold-rolled carbon steel, and unpolished galvanized steel. Comparison of the spectra between the different surfaces for each explosive shows that the effect of the substrate causes a slight shift in the resonant frequency of the VSFS transition and that in general there is a decrease in I_{SFG} for rougher surfaces. Figure 2 also demonstrates that SFG signals can be observed from surfaces that produce both specular (fused silica, polished metals) and diffuse (unpolished metals) reflections. This shows that a signal could be observed from most surfaces encountered, since all surfaces will produce a diffuse reflection. However, even I_{SFG} from polished metal surfaces shows a decrease compared to the signal from fused silica, and there is also evidence of a shift in resonant wavelength (compare the wavenumber for the maximum I_{SFG} for fused silica with galvanized steel). This suggests that there is a need to understand how substrate composition affects the VSFS response of explosives.

The objectives of the work proposed were to understand the nonlinear optical response of explosives on surfaces that are typically encountered in urban environments, determine if environmental contaminants produce signatures that would mimic those from explosives, and demonstrate that VSFG signals can be detected at stand-off distances of up to five meters.

The effect of substrate on VSFS response was first investigated by collecting VSFS spectra for RDX and TNT on several types of plastics. The presence of an organic substrate might contribute additional vibrational band structure to the signature of the explosives and complicate their detection. Figure 3 and Figure 4 show spectra of RDX and TNT, respectively, on several different plastic and organic polymer materials. In all cases the location of the VSFS resonances in the spectra are unaffected by the substrate. However, in some cases there is an effect of substrate on signal intensity.

The working hypothesis for why I_{SFG} is a function of substrate is related to the crystal structure of the explosive on the surface. Figure 5 shows video microphotographs of RDX crystals. The top image in Figure 5 is RDX crystals as they exist on a thin layer of material formed by evaporation of solvent containing small amounts of the pure explosive. The bottom image shows crystals grown from cooling pure liquid RDX. Figure 6 shows VSFS spectra of the two types of crystals shown in Figure 5. The spectra show that I_{SFG} for the solvent-generated crystals is a factor of 30 larger than the melt crystals.

The melt crystals are in general several orders of magnitude larger, meaning their surface area to mass ratio is small compared to the solvent-generated crystals. This in part explains the decrease in signal intensity. However, a more subtle difference is related to conformation

isomers of RDX and TNT. In the case of HMX, the crystal structure of the material was shown to have a large effect on the VSFS response and recrystallization from molten material generated crystals with a much lower I_{SFG} than crystals produced by solvent evaporation [*Surber et al.*, 2007]. RDX and TNT adopt the same types of conformational isomers as HMX, and it is possible that different polymer substrates could affect their crystal structure, leading to generation of crystals with lower VSFS response. Additionally, in the case of TNT it is possible that different substrates prevent crystallization of TNT, leaving it in the form of small droplets on the surface.

The next series of measurements looked at the behavior of RDX on more complex substrates, including contaminants that might be found in a typical urban environment. It is known that photochemical smog produces organic compounds that have the same nitro-group functionality of explosives. If these compounds condense in appreciable amounts on surfaces, their presence would interfere with the VSFS detection of RDX, TNT, and other nitro-containing compounds.

A small smog chamber was constructed where organic vapor (octane), a small amount of automobile exhaust (to provide the oxides of nitrogen required to initial photocatalysis), and a polished T-6061 aluminum alloy plate were introduced into a sealed Teflon bag. The bag was placed in a chamber and irradiated with ultraviolet light for approximately three hours to allow formation of photochemical smog products on the aluminum plate. The plate was removed from the Teflon bag and then a small amount of RDX was placed on the plate. Figure 7 shows a VSFS spectra of RDX and photochemical smog components. For reference in Figure 7, spectra for pure RDX and RDX that has been exposed to UV light for three hours are shown. There is no appreciable change in the VSFS response of RDX, and there is no evidence that atmospheric oxidation products provide a chemical interference. Figure 8 shows the spatial distribution of the VSFS signal on the aluminum plate, and the main influence of the smog products is to increase the spatial variability of the signal.

Figure 9 shows RDX deposited on an aluminum plate containing adipic acid . Adipic acid represents an organic acid such as might be found in animal oils or fats. As in the case for the smog products, the signal for RDX is readily detected, although there is significant spatial variability.

Figure 10 through Figure 13 show RDX spectra taken on aluminum plate coated with enamel paint containing black, blue, red, and yellow pigment. The chemical compositions of the pigments are not known, but they show that the chromophoric content of the substrate does not interfere with the overall VSFS signal level.

Figure 14 shows RDX deposited on an aluminum plate containing synthetic urine as the contaminant. Synthetic urine was chosen as a simulant for reduced nitrogen species, which are commonly found in urban and rural environments from animal and bird droppings. There was no effect of urine on signal levels, although the distribution of RDX on the plate was nonuniform.

Figure 15 shows the spatial distribution of RDX in the presence of a light-weight hydrocarbon-based oil. As in all other cases, there was no effect of the contaminant on the VSFS signal level.

The ability of VSFS to function in a stand-off configuration was addressed using the instrumental configuration shown in Figure 16. The critical feature of this setup was the co-aligning of the infrared and green laser beams so that they could be directed at the target together. Furthermore, very long focal length lenses were used to provide long beam waists. The system was able to produce usable SFG signals over a target distance

of 0.12 m, which is contrast to laboratory configurations where target distances must be set to within a hundred microns at the most.

Figure 17 shows VSFS signal intensities measured from a series of five suitcases containing trace levels of urea that were moving on a baggage conveyor past the interrogation region. The speed of the conveyor belt was 0.5 m s^{-1} and given the approximate size of each bag as 0.5 m resulted in less than a second for detection of the contaminant. The data show that the method was able to detect urea on the luggage, showing that VSFS can be used as a rapid stand-off probe [*Asher and Willard-Schmoe*, 2013; *Asher et al.*, 2013a].

Figures

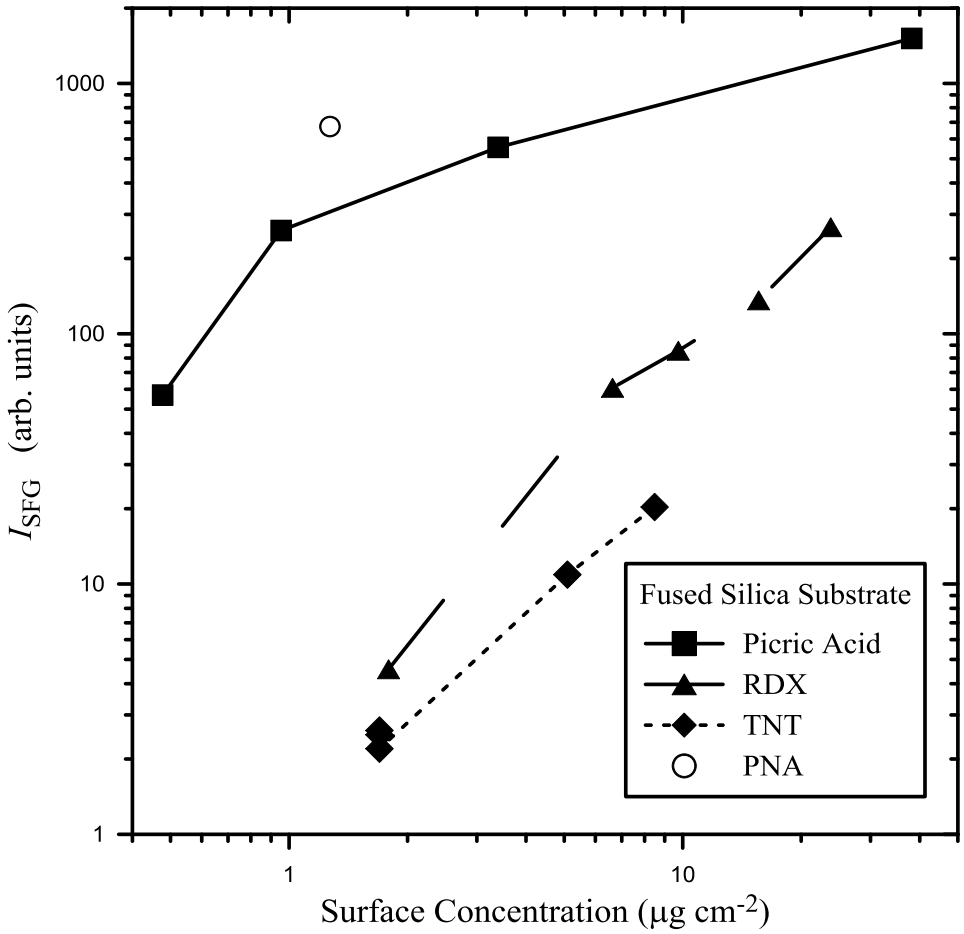

Figure 1: Vibrational sum-frequency generation signal intensities, I_{SFG}, plotted as a function of surface concentration for the explosives picric acid, RDX, and TNT on a fused silica substrate measured by *Asher et al.* [2013b]. Also shown for reference is I_{SFG} for the reference compound *p*-nitroaniline (PNA). I_{SFG} = 1 represents the lowest surface concentration that would be reliably detected above the background value.

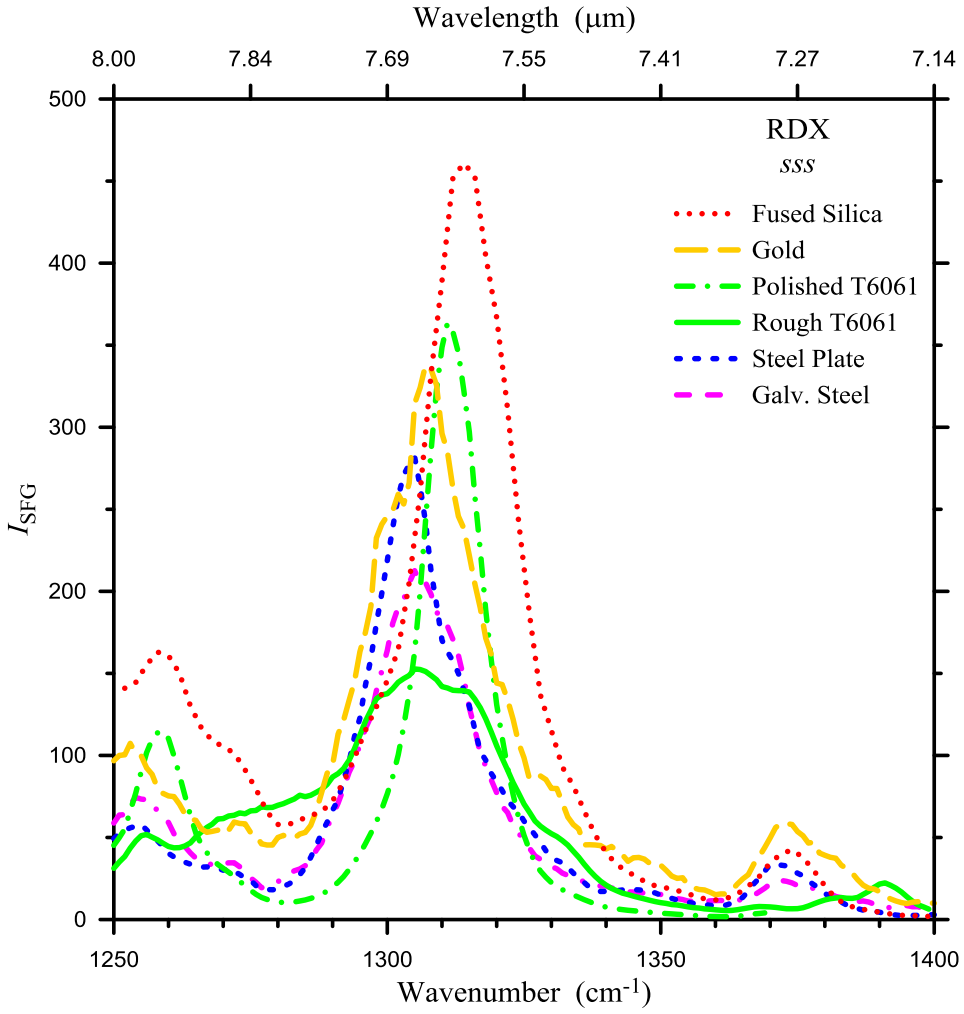

Figure 2. Vibrational sum-frequency spectra of thin films of RDX adsorbed on fused silica, gold, polished and rough T6061 aluminum, cold-rolled carbon steel plate, and galvanized steel plate. VSFS signal intensities, I_{SFG},, has been normalized to constant incident laser power for each spectra. Surface concentration of RDX was approximately 20 μg cm^{-2} for each spectra.

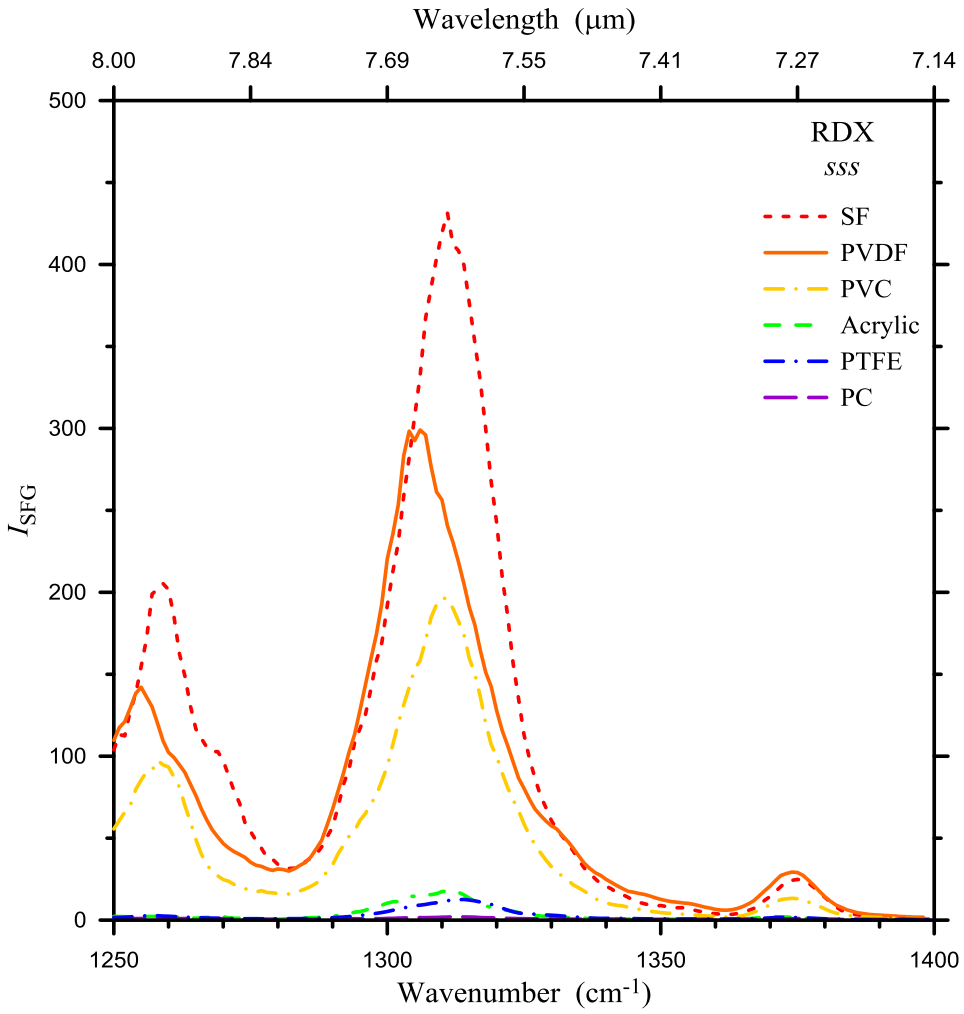

Figure 3. VSFS spectra of RDX on plastic and polymer composite material. SF: Structural fiberglass phenolic resin; PVDF: polyvinyldifluoride; PVC: polyvinylchloride; Acrylic: polymethyl methacrylate; PTFE: polytetrafluoroethylene; PC: polycarbonate. VSFS signal intensities, I_{SFG},, has been normalized to constant incident laser power for each spectra. Surface concentration of RDX was approximately 20 μg cm^{-2} for each spectra.

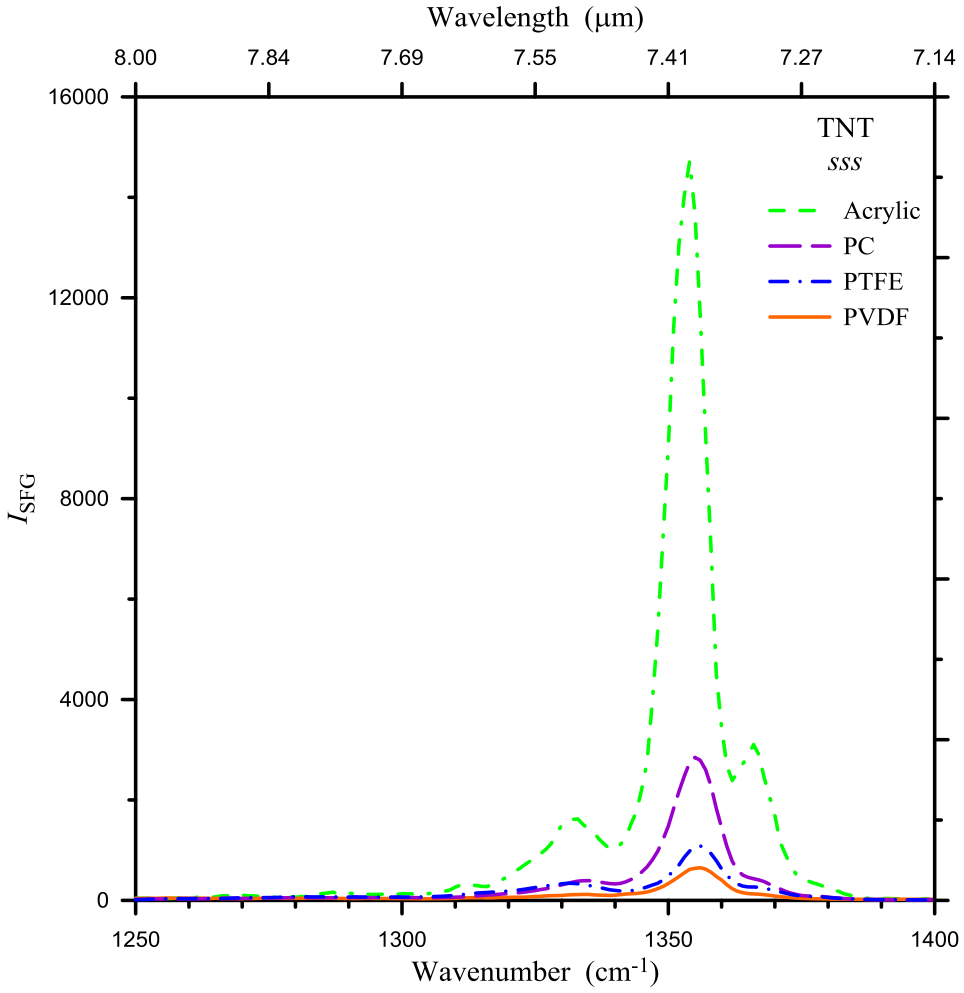

Figure 4. VSFS spectra of TNT on plastic and polymer composite material. PVDF: polyvinyldifluoride; Acrylic: polymethyl methacrylate; PTFE: polytetrafluoroethylene; PC: polycarbonate. VSFS signal intensities, I_{SFG},, has been normalized to constant incident laser power for each spectra. Surface concentration of TNT was approximately 15 μg cm^{-2} for each spectra.

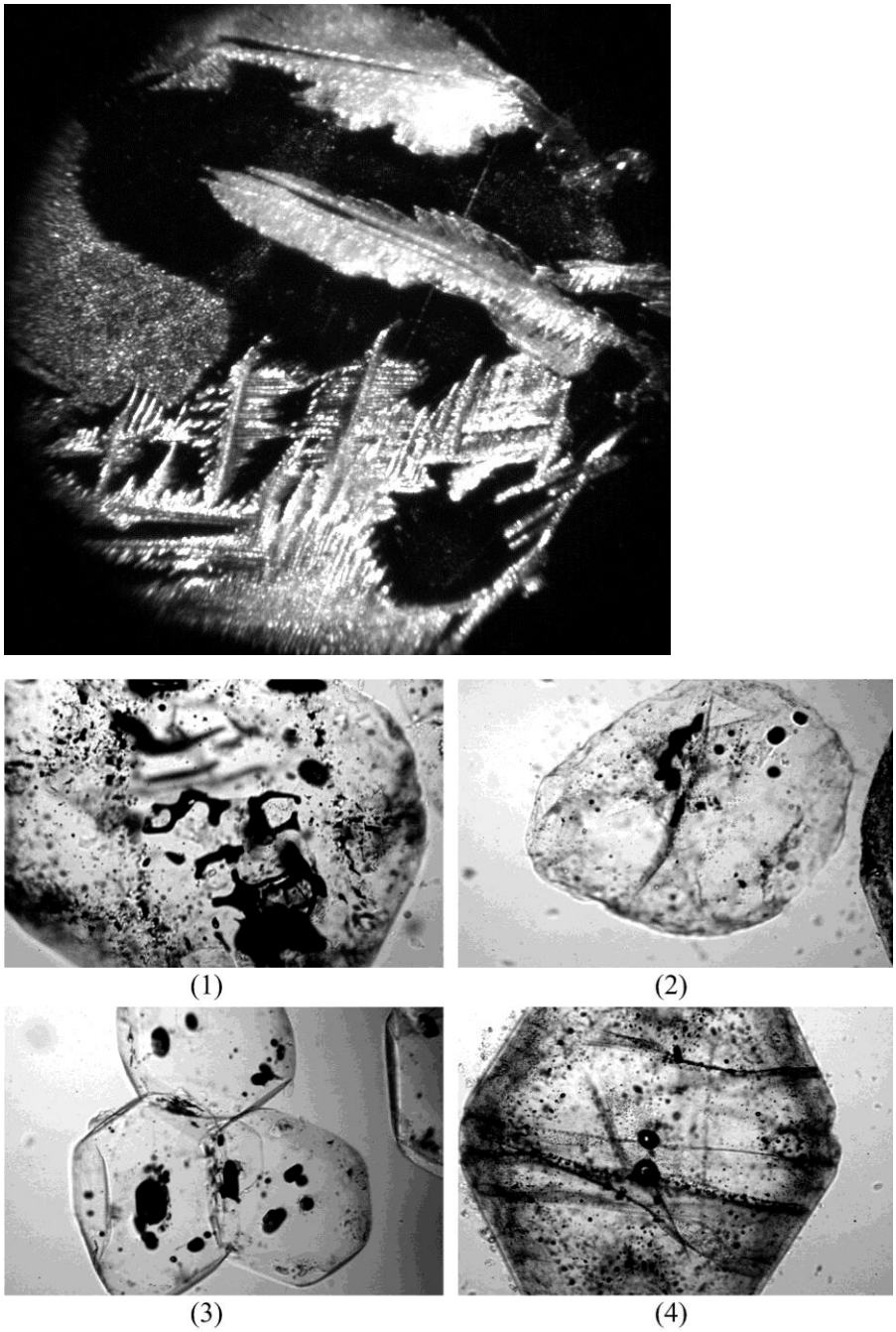

Figure 5. RDX crystals. Top image: Video microphotgraph of RDX crystals grown by recrystallization from an evaporating drop of RDX dissolved methanol. Bottom image: RDX crystals grown by recrystallization from liquefied pure RDX. Top scale: 1 cm = 70 microns, bottom scale 1 cm = 500 microns.

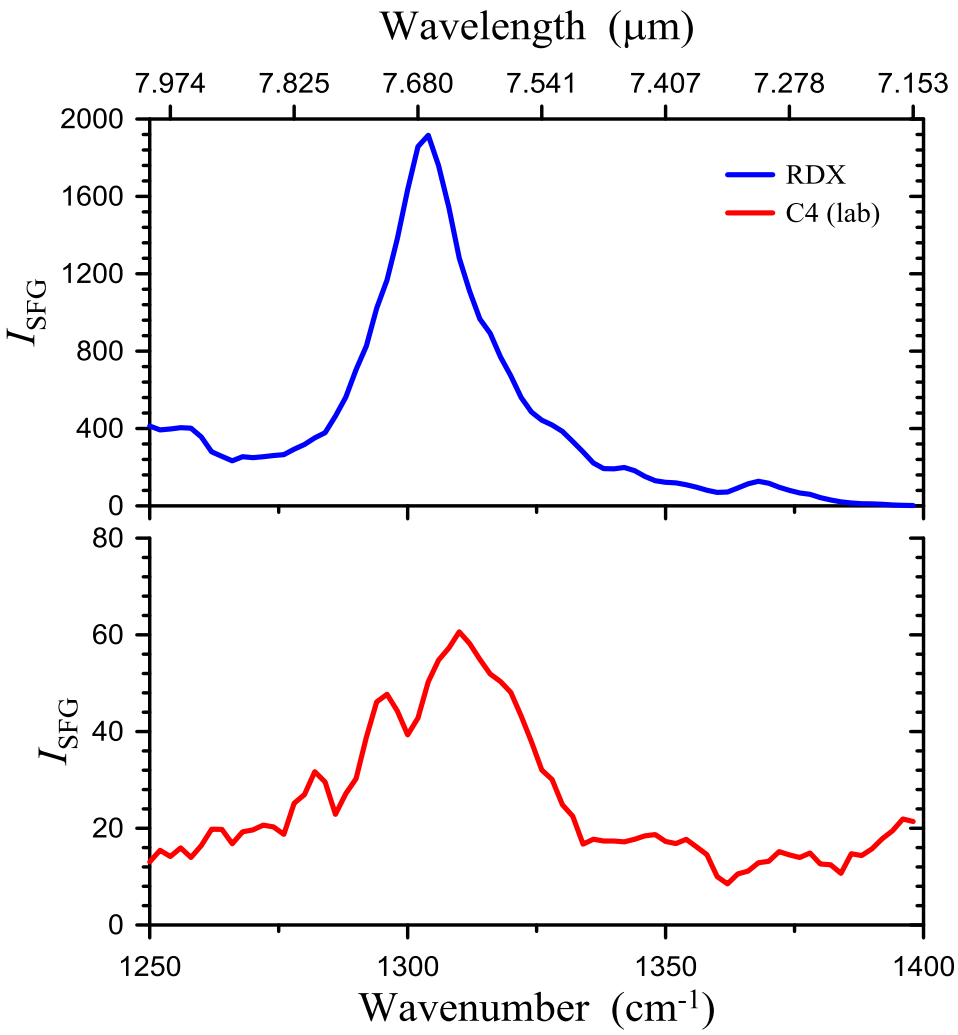

Figure 6. VSFS spectra of RDX and C4 on brushed-finish T-6061 aluminum alloy showing the decrease in signal intensity for C4 compared to the response of RDX crystals formed by evaporation of pure material dissolved in methanol. VSFS signal intensities, I_{SFG},, has been normalized to constant incident laser power for each spectra. Surface concentrations of RDX and C4 were approximately 50 μg cm^{-2} for each spectra.

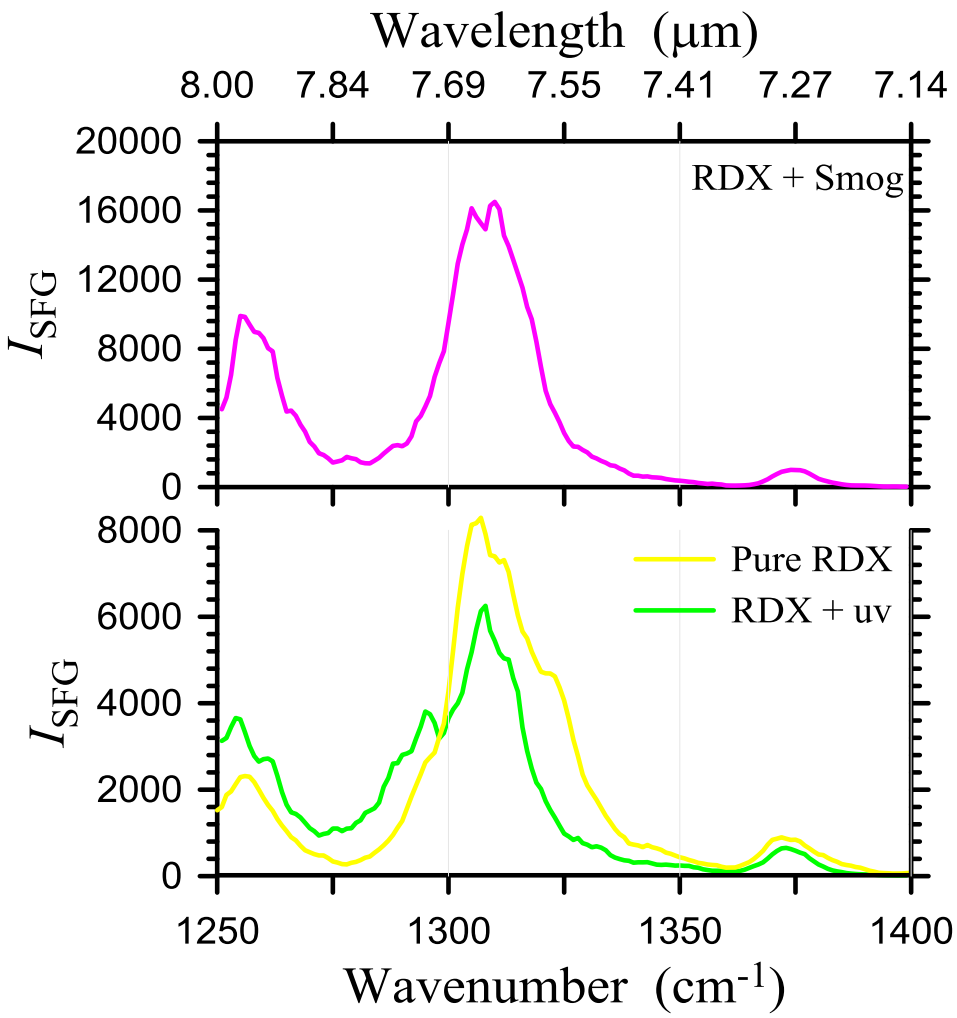

Figure 7. VSFS spectra of RDX on polished T-6061 aluminum alloy. The top spectra shows RDX that has been deposited on top of a surface exposed to photochemical smog products. The bottom spectra show spectra for pure RDX and RDX that has been exposed to ultraviolet light for a period of 3 hrs (RDX + uv). VSFS signal intensities, I_{SFG},, has been normalized to constant incident laser power for each spectra. RDX surface concentration was approximately 10 μg cm^{-2}.

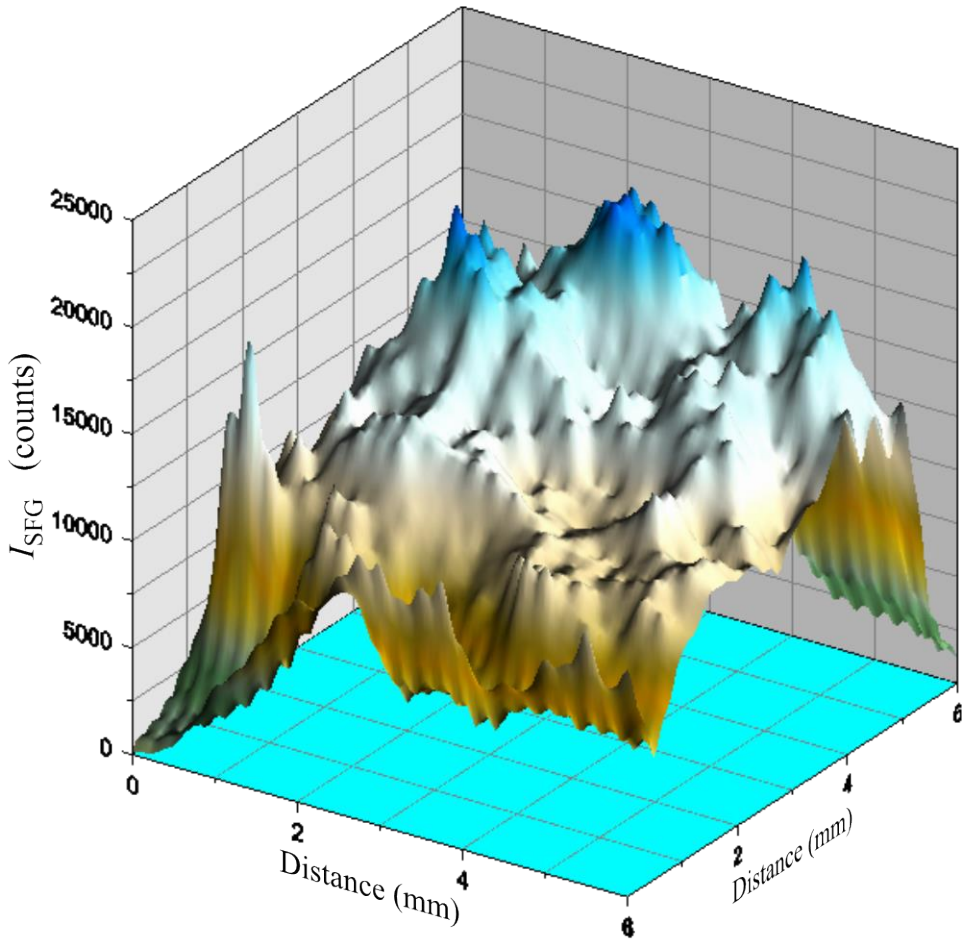

Figure 8. Spatial distribution of the VSFS response of RDX deposited on a polished T-6061 aluminum alloy surface in the presence of photochemical smog products. VSFS signal intensities, I_{SFG},, has been normalized to constant incident laser power for each spectra. RDX surface concentration was approximately 10 μg cm^{-2}.

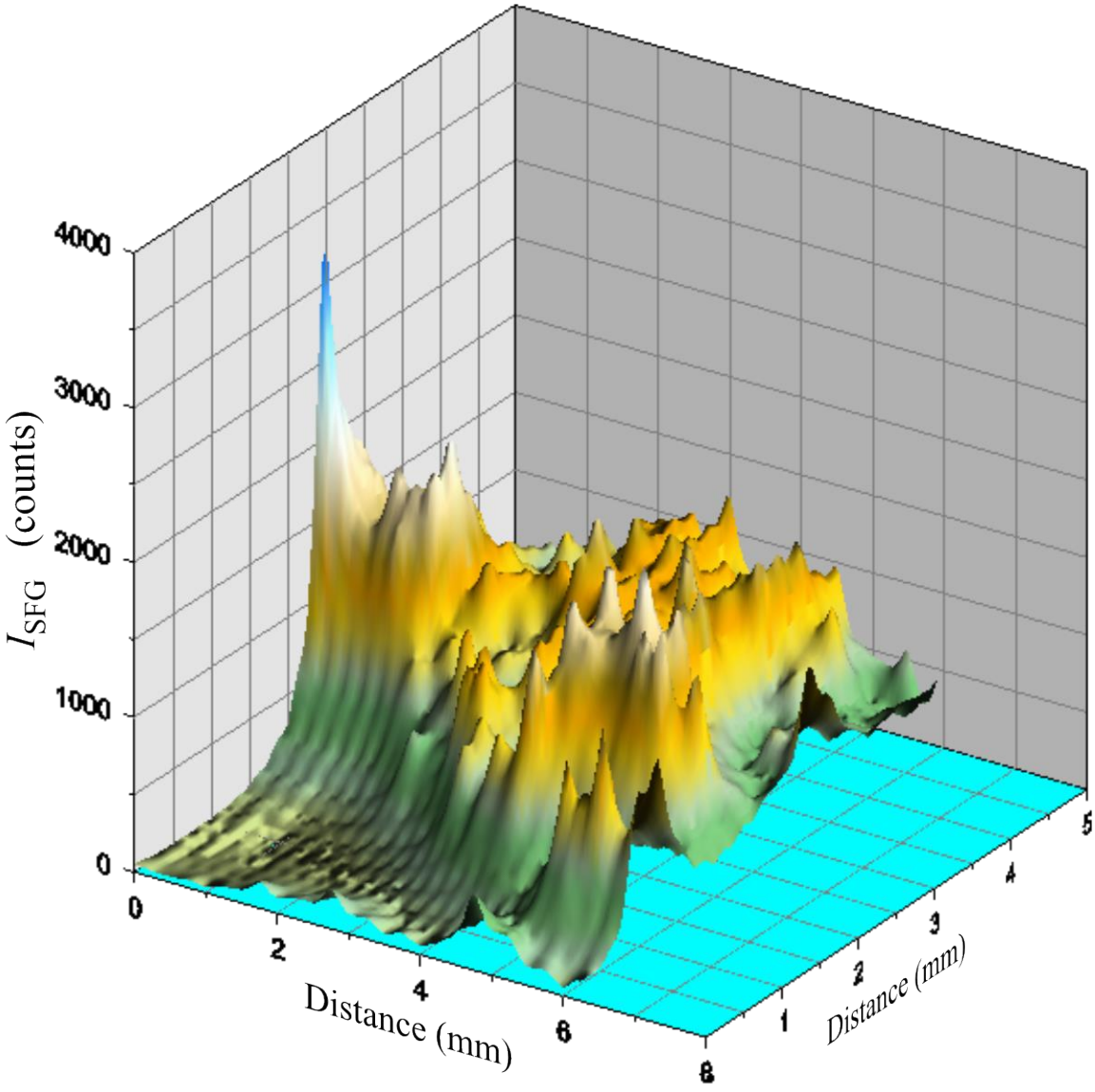

Figure 9. Spatial distribution of the VSFS response of RDX deposited on a polished T-6061 aluminum alloy surface that has been contaminated with 100 μg cm^{-2} of adipic acid. VSFS signal intensities, I_{SFG},, has been normalized to constant incident laser power for each spectra. RDX surface concentration was approximately 10 μg cm^{-2}.

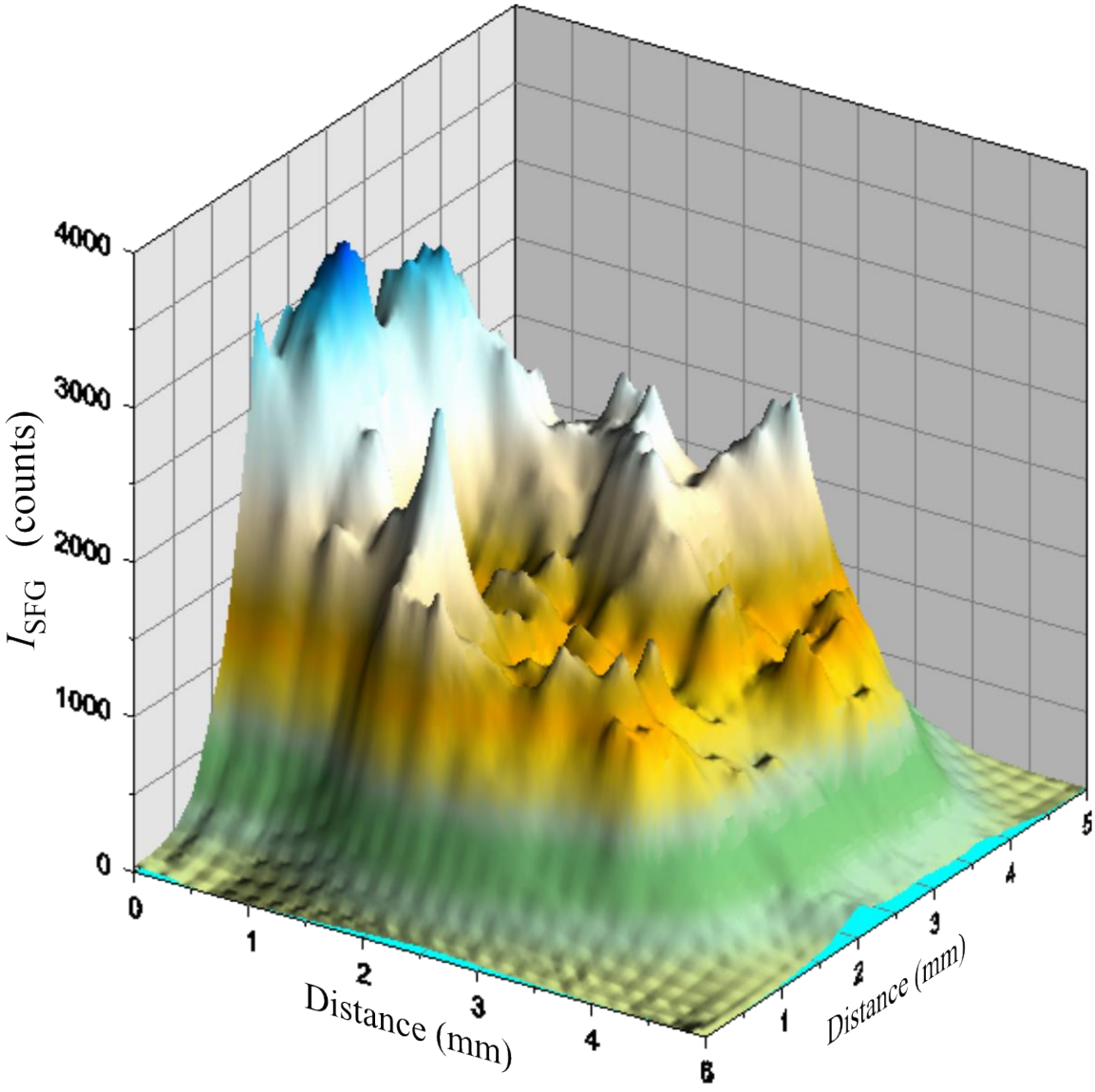

Figure 10. Spatial distribution of the VSFS response of RDX deposited on a T-6061 aluminum alloy surface that has been coated with a 1 mm thick layer of enamel paint containing black pigment. VSFS signal intensities, I_{SFG},, has been normalized to constant incident laser power for each spectra. RDX surface concentration was approximately 10 μg cm^{-2}.

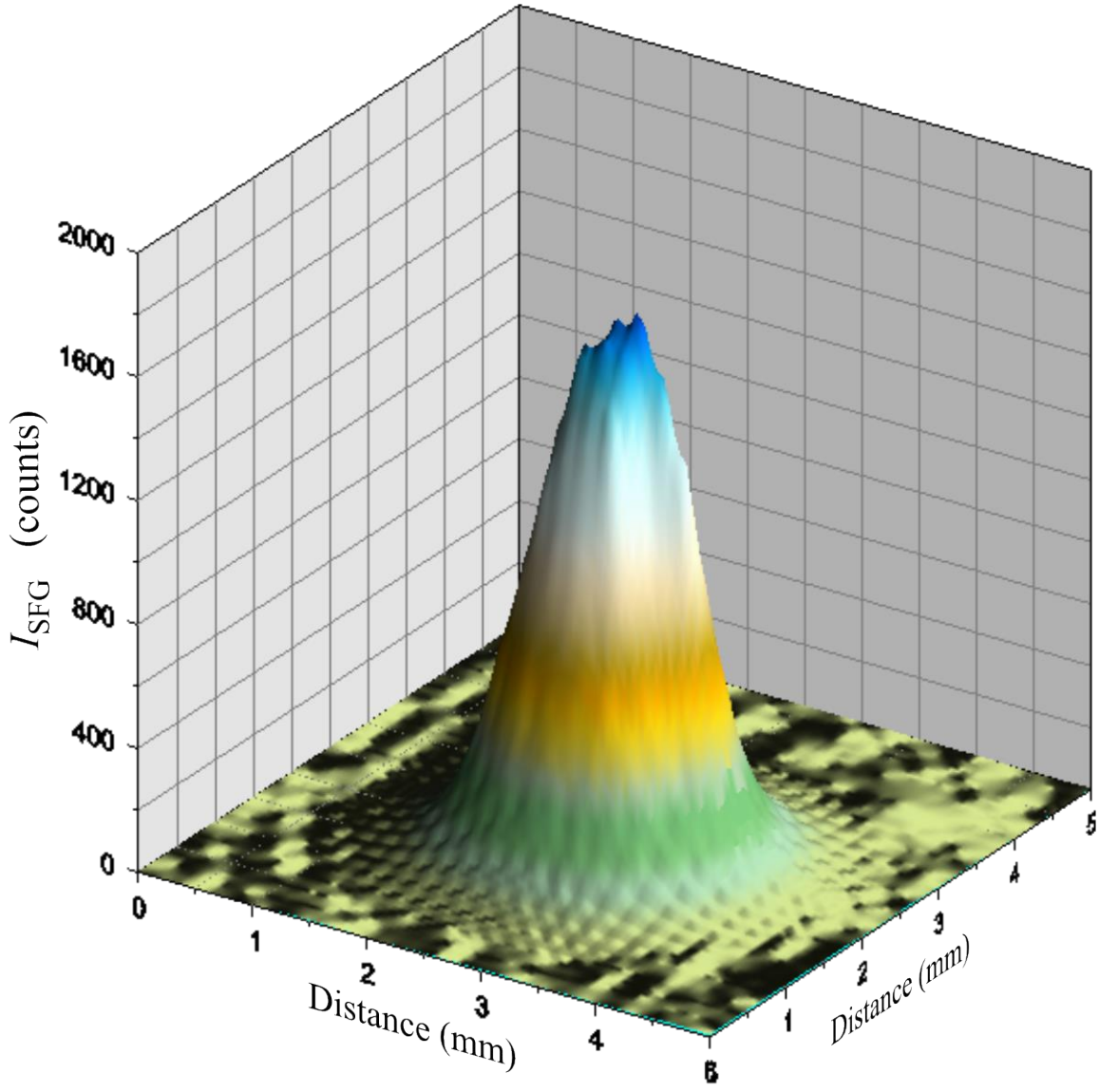

Figure 11. Spatial distribution of the VSFS response of RDX deposited on a T-6061 aluminum alloy surface that has been coated with a 1 mm thick layer of enamel paint containing blue pigment. VSFS signal intensities, I_{SFG},, has been normalized to constant incident laser power for each spectra. RDX surface concentration was approximately 10 μg cm^{-2}.

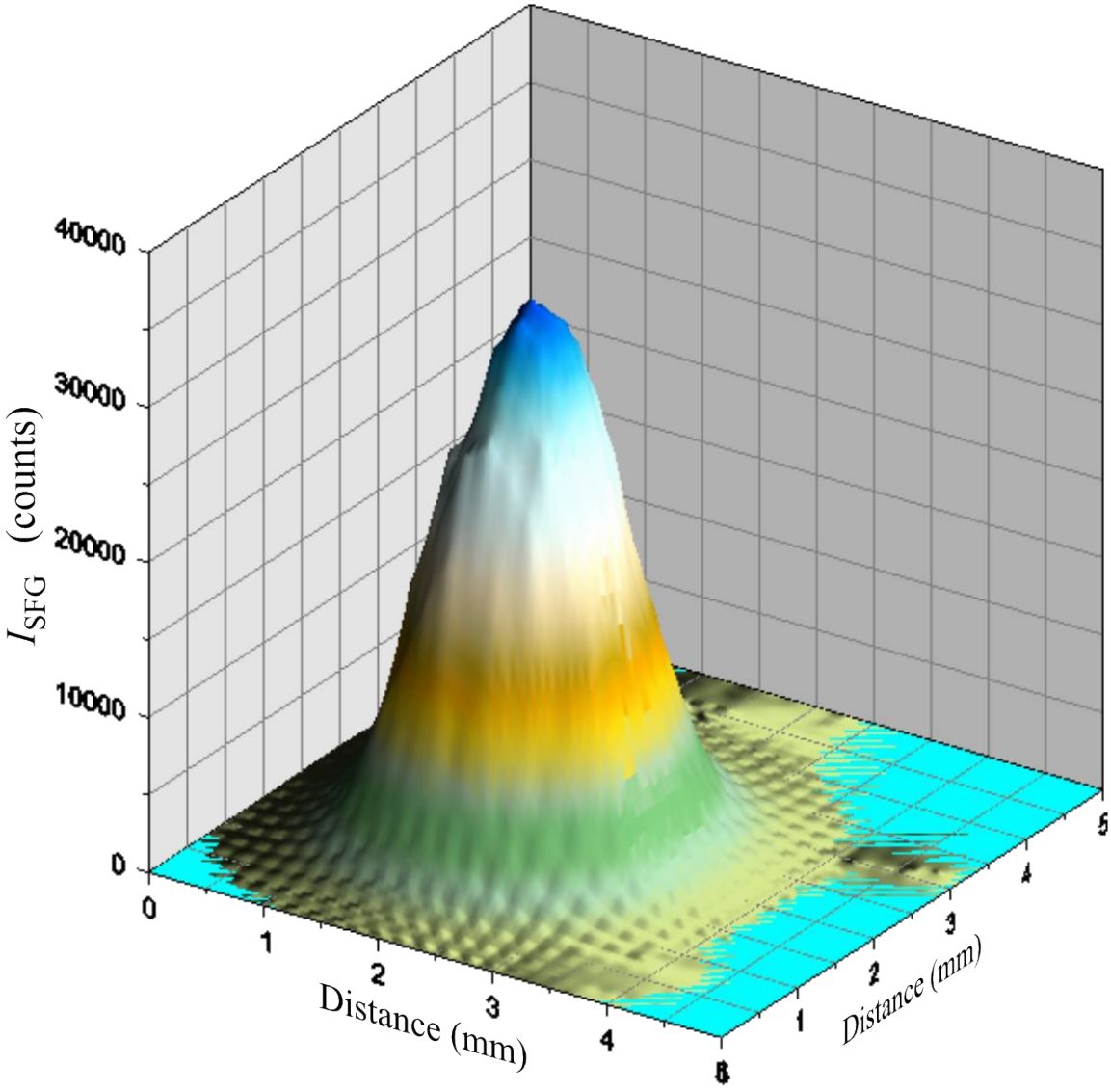

Figure 12. Spatial distribution of the VSFS response of RDX deposited on a T-6061 aluminum alloy surface that has been coated with a 1 mm thick layer of enamel paint containing red pigment. VSFS signal intensities, I_{SFG},, has been normalized to constant incident laser power for each spectra. RDX surface concentration was approximately 10 μg cm^{-2}.

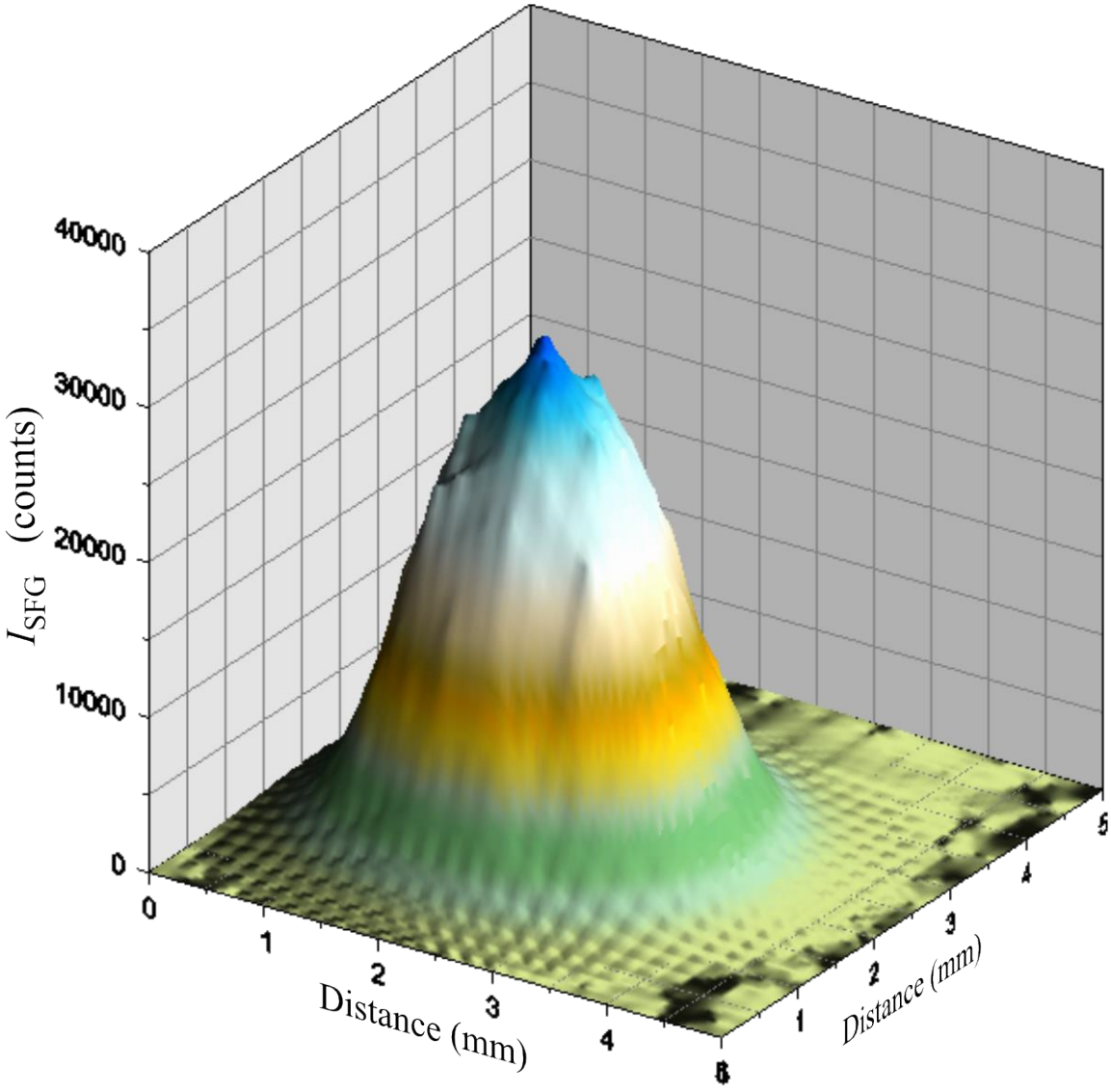

Figure 13. Spatial distribution of the VSFS response of RDX deposited on a T-6061 aluminum alloy surface that has been coated with a 1 mm thick layer of enamel paint containing yellow pigment. VSFS signal intensities, I_{SFG},, has been normalized to constant incident laser power for each spectra. RDX surface concentration was approximately 10 μg cm^{-2}.

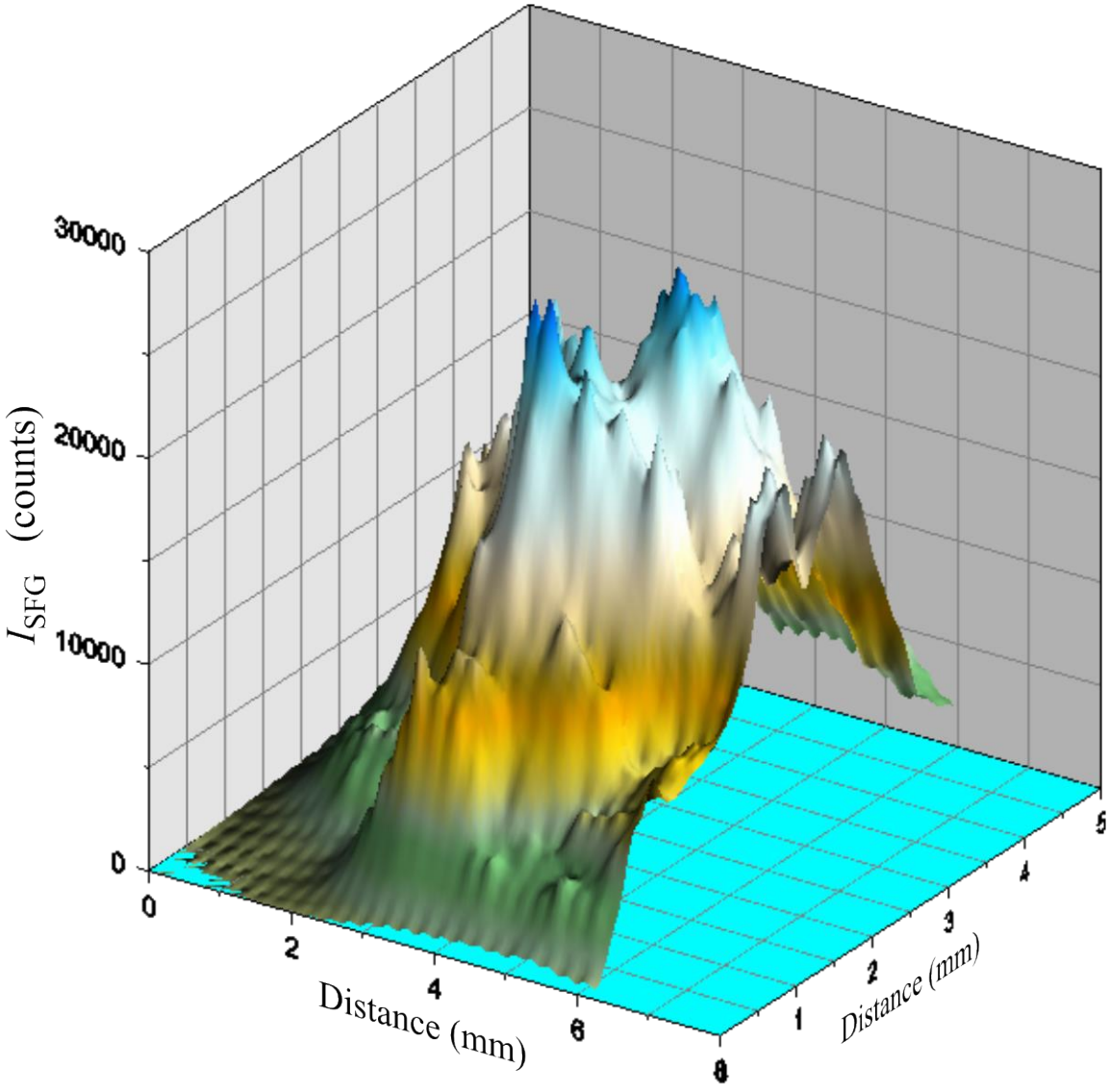

Figure 14. Spatial distribution of the VSFS response of RDX deposited on a T-6061 aluminum alloy surface that has been coated with 100 μg cm^{-2} of synthetic urine. VSFS signal intensities, I_{SFG},, has been normalized to constant incident laser power for each spectra. RDX surface concentration was approximately 10 μg cm^{-2}.

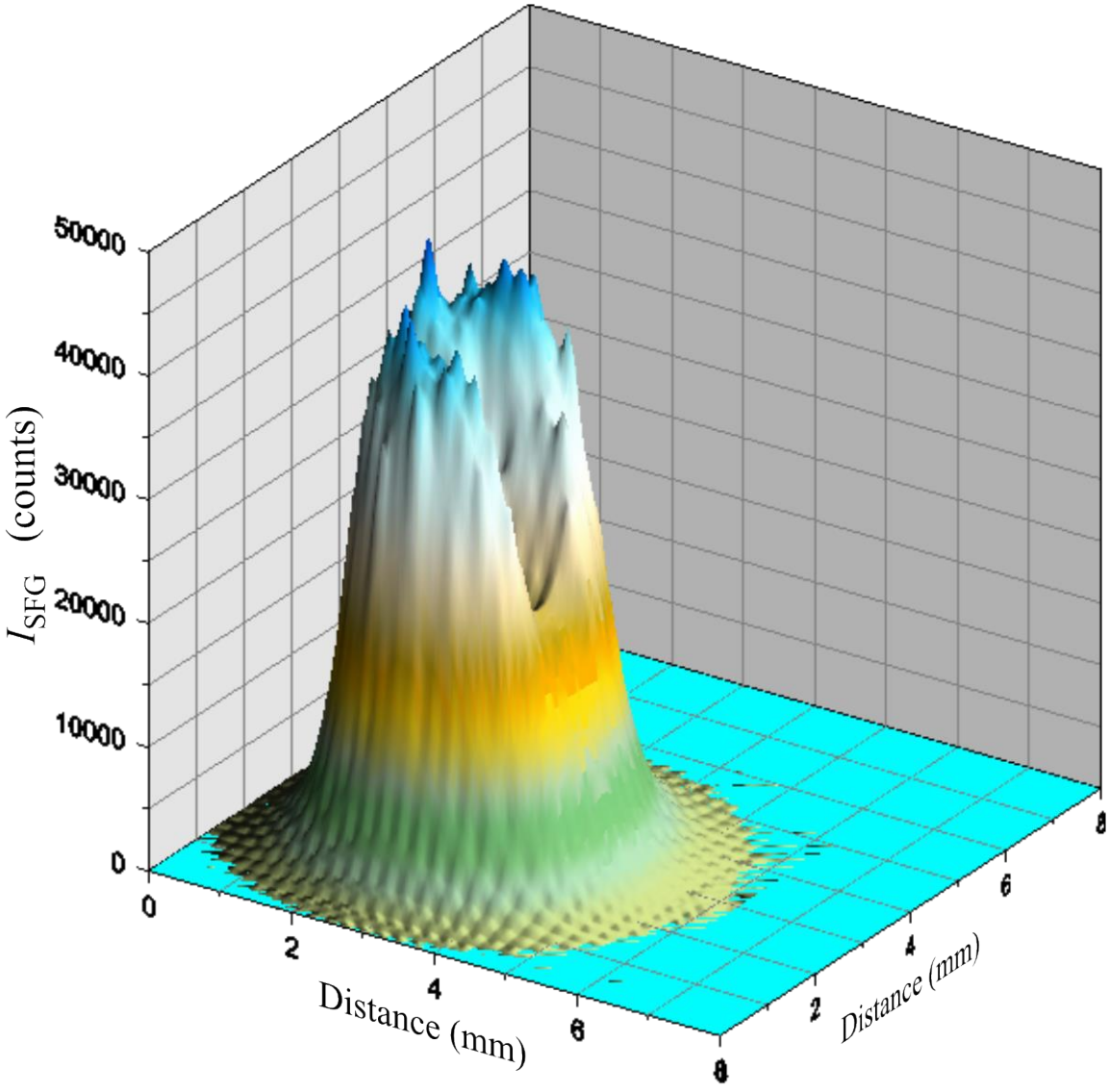

Figure 15. Spatial distribution of the VSFS response of RDX deposited on a T-6061 aluminum alloy surface that has been coated with 100 μg cm^{-2} of a light oil. VSFS signal intensities, I_{SFG},, has been normalized to constant incident laser power for each spectra. RDX surface concentration was approximately 10 μg cm^{-2}.

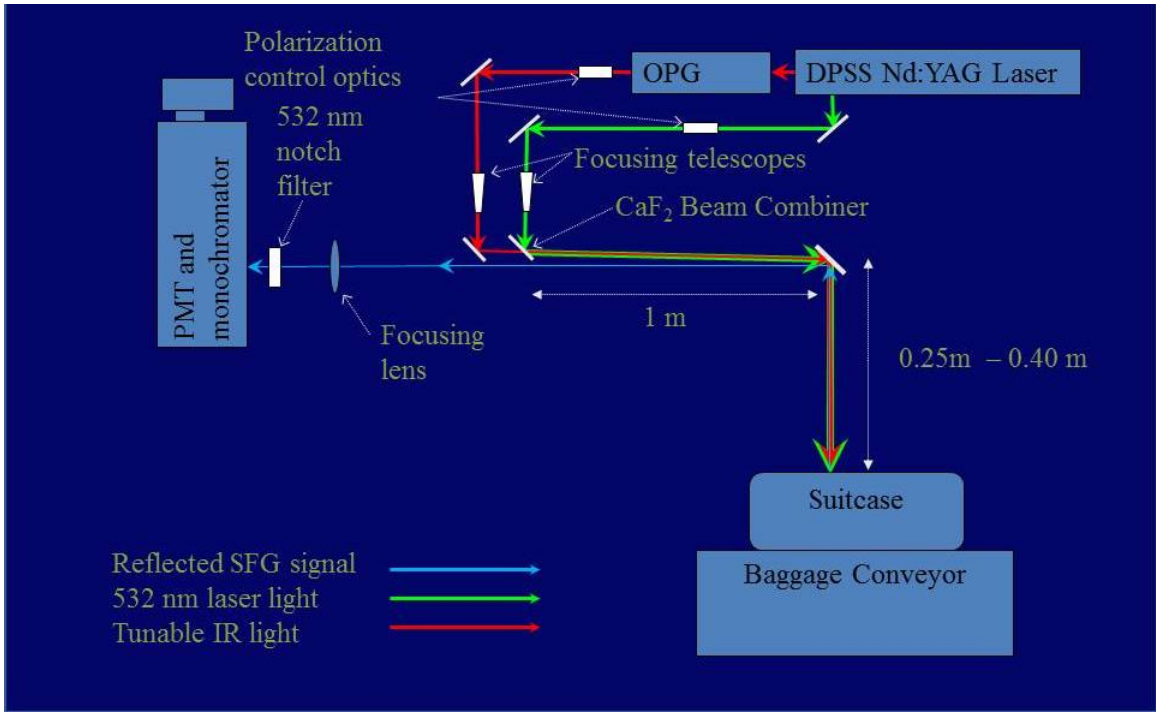

Figure 16. Schematic diagram of the VSFS configuration used to conduct the stand-off tests on a moving luggage carousel.

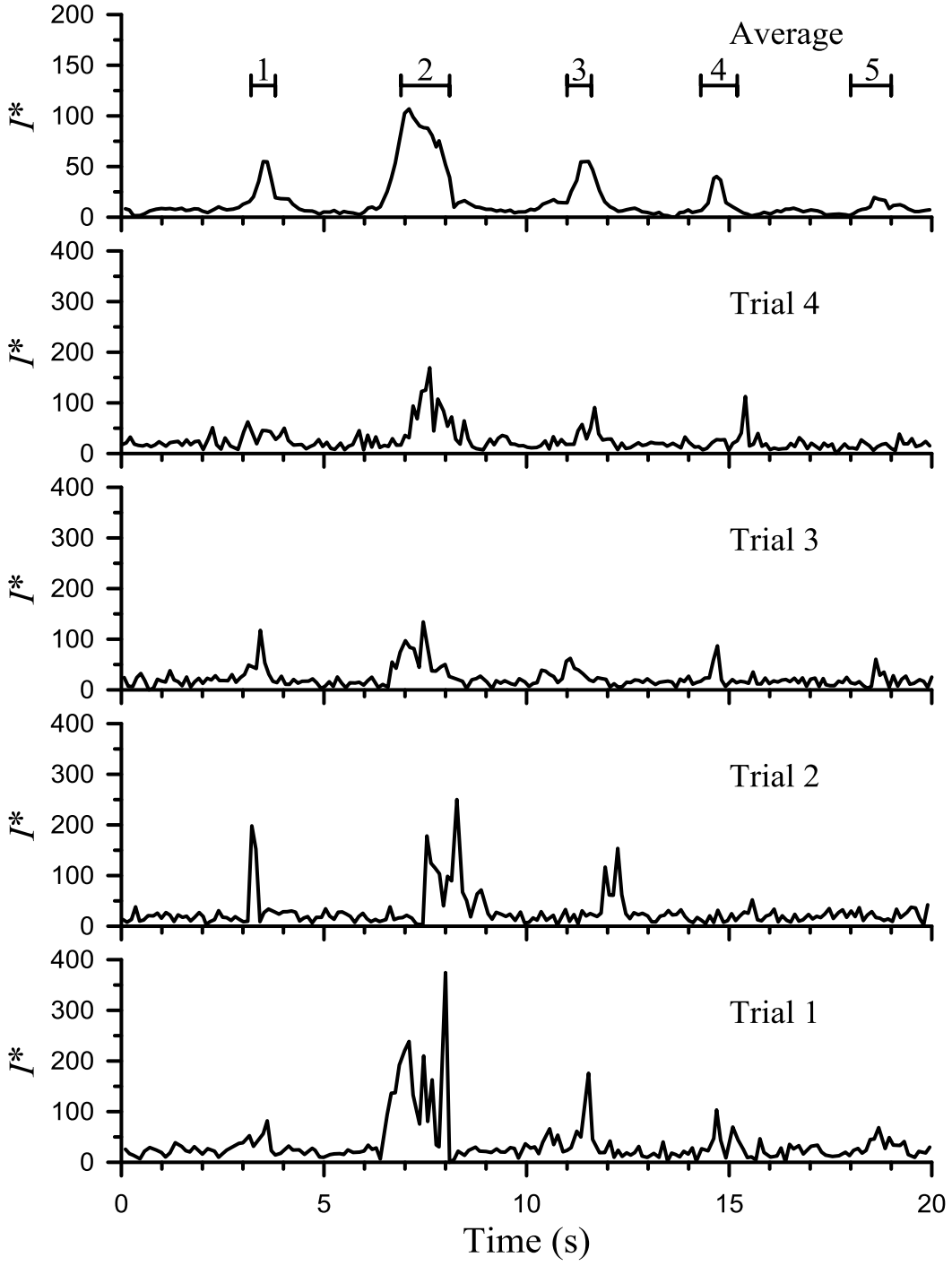

Figure 17. Time series of VSFS response from five suitcases contaminated with urea at surface mass concentrations on order of 20 μg cm^{-2}. The lower four time series shows data show four individual trials and the top-most time series is the average of the four trials.

Final Report for ONR CODE 30 SAAET Program

10. **Deliverables, Personnel, Awards, Publications, Presentations, and Patents**

Deliverable	Date
Asher, W. E., and E. Willard-Schmoe (2010), Vibrational sum frequency spectroscopy for stand-off detection of chemicals on surfaces, paper presented at FACSS 2010, Raleigh-Durham.	2010
Asher, W. E., and E. Willard-Schmoe (2013), Vibrational sum frequency spectroscopy for trace chemical detection on surfaces at stand-off distances, Appl. Spect., 67(3), 253-260.	2013
Asher, W. E., G. S. Witkop, and E. Willard-Schmoe (2013), Range insensitive optical configurations for vibrational sum frequency spectroscopy: Application to rapid screening of baggage for trace explosives, Appl. Spect., submitted.	2013
Asher, W. E., E. Willard-Schmoe, and A. Spott (2013), The vibrational sum-frequency spectra of films of picric acid, RDX, and TNT on solid surfaces, Appl. Spect., in preparation.	2013

Table 1. Deliverables

Final Report for ONR CODE 30 SAAET Program

	Total #	Name	Organization
PIs	1	William Asher	APL-UW
Co-PIs	1	Dale Winebrenner	APL-UW
Grad Students	0		
Post Docs	0		
Research Assistants	1	Ella Willard-Schmoe	APL-UW

Table 2. Personnel Information

Final Report for ONR CODE 30 SAAET Program

	Name	Award (Year Received)	Prize (Year Received)	Recognition (Year Received)
PIs	William Asher	none	none	none
Co-PIs	Dale Winebrenner	none	none	none
Grad Students	N/A			
Post Docs	N/A			
Research Assistants	Ella Willard-Schmoe	none	none	none

Table 3. Awards/Prizes/Recognitions

Name	Publication (Date)	Conference Presentation (Date)	Patent (Date)
William Asher	2013(1), 2013(2)		

Table 4. Publications, Conference Presentations and Patents

Final Report for ONR CODE 30 SAAET Program

11. **References:** (In support of Sections 7-9 above.)

Asher, W. E., and E. Willard-Schmoe (2013), Vibrational sum frequency spectroscopy for trace chemical detection on surfaces at stand-off distances, *Appl. Spect.*, *67*(3), 253-260.

Asher, W. E., G. S. Witkop, and E. Willard-Schmoe (2013a), Range insensitive optical configurations for vibrational sum frequency spectroscopy: Application to rapid screening of baggage for trace explosives, *Appl. Spect.*, *submitted*.

Asher, W. E., E. Willard-Schmoe, and A. Spott (2013b), The vibrational sum-frequency spectra of films of picric acid, RDX, and TNT on solid surfaces, *Appl. Spect.*, *in preparation*.

CREPSEDT (2004), Existing and Potential Standoff Explosives Detection Techniques*Rep.*, 148 pp, National Academy Press, Washington D.C.

Fidric, B. G., R. A. Provencal, S. M. Tan, E. R. Crosson, A. A. Kachanov, and B. A. Paldus (2003), Bananas, explosives and the future of cavity ring-down spectroscopy, *Opt. Phot. News*, *14*, 24-29.

Gan, W., B.-H. Wu, Z. Zhang, Y. Guo, and H.-F. Wang (2007), Vibrational Spectra and Molecular Orientation with Experimental Configuration Analysis in Surface Sum Frequency Generation (SFG), *J. Phys. Chem. C*, *111*(12), 8716-8725.

Heinz, T. F., H. W. K. Tom, and Y. R. Shen (1983), Determination of Molecular-Orientation of Monolayer Adsorbates by Optical 2nd-Harmonic Generation, *Phys. Rev. A*, *28*, 1883-1885.

Hunt, J. H., P. Guyot-Sionnest, and Y. R. Shen (1987), Observation of C-H stretch vibrations of monolayers of molecules optical sum-frequency generation, *Chem. Phys. Lett.*, *133*, 189-192.

Lambert, A. G., P. B. Davies, and D. J. Neivandt (2005), Implementing the theory of sum frequency generation vibrational spectroscopy: A tutorial review, *Appl. Spec. Rev.*, *40*(2), 103-145.

Shen, Y. R. (1984), *The Principles of Nonlinear Optics*, 612 pp., J. Wiley, New York.

Shen, Y. R. (1999), Surface contribution versus bulk contribution in surface nonlinear optical spectroscopy, *Appl. Phys. B*, *68*(3), 295-300.

Shen, Y. R. (2000), Surface nonlinear optics: A historical perspective, *IEEE J. Sel. Topics Quant. Elec.*, *6*(6), 1375-1379.

Stott, W. R., D. Green, and A. G. Mercado (1994), Mass spectrometric detection of solid and vapor explosive materials, *Proc. SPIE*, *2276*(Cargo Detection Technologies), 87-97.

Surber, E., A. Lozano, A. Lagutchev, H. Kim, and D. D. Dlott (2007), Surface nonlinear vibrational spectroscopy of energetic materials: HMX, *J. Phys. Chem. C*, *111*, 2235-2241.

Wang, H.-F., W. Gan, R. Lu, Y. Rao, and B. H. Wu (2005), Quantitative spectral and orientational analysis in surface sum frequency generation vibrational spectroscopy (SFG-VS), *Int. Rev. Phys. Chem.*, *24*(2), 191-256.

Zhuang, X., P. B. Miranda, D. Kim, and Y. R. Shen (1999), Mapping molecular orientation and conformation at interfaces by surface nonlinear optics, *Phys. Rev. B*, *59*, 12632-12640.

Zyss, J. (1993), Engineering new organic crystals for nonlinear optics: from molecules to oscillator, *J. Phys. D*, *26*, B198-B207.

REPORT DOCUMENTATION PAGE

Form Approved
OMB No. 0704-0188

PLEASE DO NOT RETURN YOUR FORM TO THE ABOVE ADDRESS.

1. REPORT DATE *(DD-MM-YYYY)*	2. REPORT TYPE	3. DATES COVERED *(From - To)*
4 November 2013	Final Technical Report	01-Jun-2009 -- 30-Sep-2013

4. TITLE AND SUBTITLE

Understanding Chemical Sensitivity and Surface Response in Detecting Trace Levels of Explosives Using Vibrational Sum Frequency Spectroscopy

5a. CONTRACT NUMBER

5b. GRANT NUMBER

N00014-09-1-0983

5c. PROGRAM ELEMENT NUMBER

6. AUTHOR(S)

William Asher, University of Washington

5d. PROJECT NUMBER

5e. TASK NUMBER

5f. WORK UNIT NUMBER

7. PERFORMING ORGANIZATION NAME(S) AND ADDRESS(ES)

Applied Physics Laboratory
University of Washington
1014 NE 40th St.
Seattle, WA 98105

8. PERFORMING ORGANIZATION REPORT NUMBER

9. SPONSORING/MONITORING AGENCY NAME(S) AND ADDRESS(ES)

Michael F. Shlesinger Code 30
Office of Naval Research
875 North Randolph Street
Arlington, VA 22203

10. SPONSOR/MONITOR'S ACRONYM(S)

ONR

11. SPONSOR/MONITOR'S REPORT NUMBER(S)

12. DISTRIBUTION/AVAILABILITY STATEMENT

Distribution Statement A: Approved for public release, distribution unlimited.

13. SUPPLEMENTARY NOTES

14. ABSTRACT

Vibrational sum frequency spectroscopy (VSFS) can be used to detect trace quantities of high explosives (HEs) adsorbed on surfaces. As a trace detection method, VSFS has the advantages of being non-contact and non-destructive with sub-second detection times. Therefore, a HE-detection method for detecting IEDs or portal defense that was based on VSFS could provide stand-off trace detecting for IEDs and increase the throughput of package screening (in terms of objects scanned per minute) for portal defense. Furthermore, because VSFS does not degrade contaminants on surfaces, a positive detection result leaves any explosives detected in place for subsequent forensic analysis such as fingerprint identification. This research has shown that that VSFS provides high chemically selectivity for nitro-containing HEs in the presence of environmental chemical contaminants. The

by the scintillation index, is exponential: ˙2(t) 12 exp(• • t)ln(1= h) + 1 + (

quantum signature of classical chaos.

• • 1ln(1= h). The approach toward equilibrium, as me

by the scintillation index, is exponential: ˙2(t) 12 exp(• • t)ln(1= h) + 1 + O(h=t2). This provides a

15. SUBJECT TERMS

vibrational sum frequency spectroscopy (VSFS), high explosives (HEs), improvised explosive devices (IEDs)

16. SECURITY CLASSIFICATION OF:			17. LIMITATION OF ABSTRACT	18. NUMBER OF PAGES	19a. NAME OF RESPONSIBLE PERSON
a. REPORT	b. ABSTRACT	c. THIS PAGE			William Asher
U	U	U	U	30	19b. TELEPHONE NUMBER *(Include area code)* (206) 616-7558

Reset